



Simulation of the enhanced infrared photoresponse of type-II GaSb/GaAs quantum ring solar cells

M. C. Wagener, P. J. Carrington, J. R. Botha, and A. Krier

Citation: [Applied Physics Letters](#) **103**, 063902 (2013); doi: 10.1063/1.4818126

View online: <http://dx.doi.org/10.1063/1.4818126>

View Table of Contents: <http://scitation.aip.org/content/aip/journal/apl/103/6?ver=pdfcov>

Published by the [AIP Publishing](#)

Articles you may be interested in

[Hybrid type-I InAs/GaAs and type-II GaSb/GaAs quantum dot structure with enhanced photoluminescence](#)
Appl. Phys. Lett. **106**, 103104 (2015); 10.1063/1.4914895

[Photocapacitance study of type-II GaSb/GaAs quantum ring solar cells](#)
J. Appl. Phys. **115**, 014302 (2014); 10.1063/1.4861129

[Enhanced infrared photo-response from GaSb/GaAs quantum ring solar cells](#)
Appl. Phys. Lett. **101**, 231101 (2012); 10.1063/1.4768942

[Type-II GaSb/GaAs coupled quantum rings: Room-temperature luminescence enhancement and recombination lifetime elongation for device applications](#)
Appl. Phys. Lett. **101**, 031906 (2012); 10.1063/1.4737443

[Ga Sb/Ga As type II quantum dot solar cells for enhanced infrared spectral response](#)
Appl. Phys. Lett. **90**, 173125 (2007); 10.1063/1.2734492

The image shows the cover of an Applied Physics Reviews journal issue. It features a 3D schematic of a quantum dot structure with various layers and labels. The text 'AIP Applied Physics Reviews' is at the top left. The background is a dark blue with a glowing light effect and a molecular structure of blue spheres.

NEW Special Topic Sections

NOW ONLINE
Lithium Niobate Properties and Applications:
Reviews of Emerging Trends

AIP Applied Physics Reviews

Simulation of the enhanced infrared photoresponse of type-II GaSb/GaAs quantum ring solar cells

M. C. Wagener,^{1,a)} P. J. Carrington,² J. R. Botha,¹ and A. Krier²

¹Department of Physics, Nelson Mandela Metropolitan University, Port Elizabeth, South Africa

²Department of Physics, Lancaster University, Lancaster LA1 4YB, United Kingdom

(Received 3 May 2013; accepted 24 July 2013; published online 6 August 2013)

The extended photo-response of solar cells containing ten periods of GaSb/GaAs quantum rings imbedded in the *p-i-n* junction has been described using a single-band representation of the type-II quantum ring structure. By fitting the experimental data, the authors were able to deduce that the quantum rings are well represented by a Gaussian height distribution and a large valence band discontinuity. The simulated band of states is shown to be well matched to the photoluminescence analysis of the structure, with the inhomogeneous size distribution resulting in a band of hole states roughly 390 meV above the valence band. © 2013 AIP Publishing LLC. [<http://dx.doi.org/10.1063/1.4818126>]

The incorporation of GaSb/GaAs quantum rings (QRs) into the junction of a GaAs solar cell has been shown to be an effective means of increasing the photocurrent of a conventional thin-film solar cell.¹ The hole confinement and the separation of the electron and hole wave-functions characteristic of type-II heterostructures (i.e., one charge carrier is localized and the QR and the other one in the barrier) leads to a range of interesting attributes, such as sub-band gap absorption and increased electron lifetimes. Although the photoluminescence (PL) properties of the various GaSb/GaAs quantum structures have been extensively reported,² there still remain some inconsistencies between the observed optical transitions and the nano-structure.³ This paper therefore sets out to relate the spectral response of the GaSb/GaAs solar cell to its structural properties, specifically the height distribution of the quantum rings.

The solar cell structure used in this study was deposited using a VG-V80H molecular beam epitaxy reactor. A detailed description of the growth procedure and the device structure is given in Ref. 1. The active region of the *p-i-n* diode contain ten layers of GaSb/GaAs QRs, with a typical surface density of 1×10^{10} rings/cm². Cross-sectional transmission electron microscopy (TEM) images showed the rings to have a typical outer and inner diameter of 23 and 10 nm, respectively, with a thickness of approximately 1.7 nm.¹ These structures were processed into circular solar cells with a diameter of 1 mm using standard photolithography (see inset in Fig. 1). The spectral response of the solar cell was determined by measuring the short-circuit photocurrent using a Keithley 6487 picoammeter and a calibrated pseudo-monochromatic light source. Appropriate long-pass filters were used to remove second-order diffraction lines.

Figure 1 shows the extended photo-response achieved when incorporating GaSb/GaAs QRs into the solar cell. The spectral response is characterised by two broad bands that have been found to scale linearly with the number of GaSb layers introduced inside the junction.¹ Both bands have

therefore been attributed to absorption by the GaSb/GaAs nano-structures, with the narrower band nearer to the GaAs absorption edge (at 1.3 eV) assigned to the wetting layer (WL) formed during the GaSb deposition. The broader band, which typically extends down to 850 meV, was ascribed to absorption by the quantum rings.

When relating the extended response of the solar cell with the structural characteristics of type-II quantum structures, various factors could affect the localization energy of holes, i.e., the geometry; the GaSb/GaAs interface composition, as well as doping effects.⁴ The relaxation of GaSb quantum dots into ring-like structures could also alter the localization energy.⁵ Comparison of various GaSb/GaAs solar cells has, however, revealed that the basic form of the extended response remained relatively insensitive to the growth mode (e.g., quantum dot *versus* quantum ring formation).⁶ Additionally, the hole effective mass, m^* , and the valence-band offset, ΔE_{VB} , also need to be known, with both parameters dependent on the residual strain within the GaSb ring.⁴

When considering the GaSb/GaAs band offsets, a range of values has been proposed. For the valence-band offset

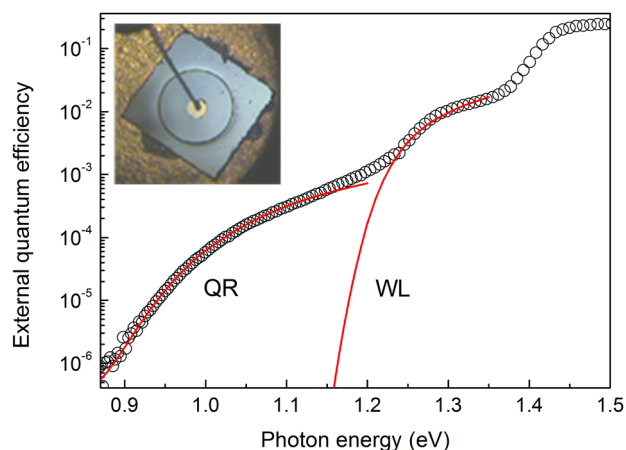


FIG. 1. Extended photo-response of a typical GaSb/GaAs solar cell (open circles). The solid lines represent the quantum rings and the wetting layers simulated using Eqs. (2) and (3). The inset depicts the device used for the photoresponse measurements.

^{a)}Author to whom correspondence should be addressed. Electronic mail: Magnus.Wagener@nmmu.ac.za

between strained GaAs and GaSb, the classical literature value of 840 meV (Refs. 7 and 8) has been disputed by the lower emission activation energies observed by deep-level transient spectroscopy (DLTS) (Ref. 3) and admittance spectroscopy.⁹ The activation energy typically displayed a strong bias dependence, probing deeper hole levels with increased band-bending. The contribution of the hole emission to the capacitance signal will, however, depend on the size distribution of the dots, with the localization energy only matching the valence band offset when quantum confinement effects become negligible. Large dots are also expected to be relaxed, with the band offset tending towards that of the natural band alignment. Additionally, the DLTS signal and associated activation energy reported by Nowozin *et al.*³ were also shown to decrease with reverse bias, suggesting that the distribution of available hole states (which corresponds to a particular height distribution) might be centered at an energy below the valence band offset. *Ab initio* calculations of the unstrained valence band offset between GaSb and GaAs has produced a range of values, with Wei and Zunger¹⁰ suggesting a low value of 570 meV and Li *et al.*¹¹ a revised value of 760 meV. Since the localization energy determined by capacitance techniques therefore appear to underestimate the valence band offset, the theoretical value of 840 meV (Refs. 7 and 8) was used as a trial value to simulate the photo-response of the GaSb quantum structures. For the QR effective hole mass, we assumed a constant value throughout the well, using the mean effective mass calculated by spatial averaging across a strained GaSb/GaAs quantum dot $m^* = 0.097m_0$.⁷ The mismatch between the effective mass of the GaAs barrier and the GaSb QR was however considered by using the BenDaniel-Duke boundary conditions¹² when calculating the QR states. Based on the strain calculations by Pryor and Pistor, we used the light hole mass of $0.082m_0$ for the GaAs barrier layer. The contribution by the WL was simulated using a GaSb/GaAs valence band offset of 980 meV and a mean effective hole mass $m^* = 0.083m_0$.⁷

The geometric dependence of the hole localization energy, E_h , in quantum rings has been intensively described using a variety of approaches, ranging from a quasi-one-dimensional representation of the QR¹³ to complex three-dimensional simulations.¹⁴ In the case of a circular ring, the ground state energy depends predominantly on the height, H , and the radial width, ΔR (outer radius minus inner radius), of the QR.¹⁴ The total energy due to confinement within the QR can then be best described by a power function¹⁴

$$E_h \sim \left(\frac{1}{H}\right)^\beta + \left(\frac{1}{\Delta R}\right)^\gamma, \quad (1)$$

where the power coefficients have been shown to be $\beta = 1/3$ and $\gamma = 1$ for a large range of QR geometries.¹⁴ When considering some variance in the QR height and ring width, the associated width of the energy distribution will primarily depend on the smaller dimension. Since $H < \Delta R$ for a variety of growth conditions and material systems,^{1,15,16} the height distribution of the rings is expected to determine the inhomogeneous broadening of the hole states, with the integrated radial confinement only offsetting the mean energy.

Preliminary values for the hole localization energies were therefore estimated using a finite potential, single-band model for the GaSb QRs, with the one-dimensional well width representing the height of the QR, and the GaSb/GaAs valence band offset the well potential. The energy distribution of the ground state could then easily be related to a particular QR height distribution, with the ΔR distribution used to offset the mean energy using Eq. (1). Following the initial simulation of the experimental photo-response, the choice of band parameters (i.e., valence band offset and effective hole mass) could be reassessed by comparing the simulated QR height and hole energy distributions, with the TEM and PL results obtained for the solar cells.

In the case of the type-II GaSb/GaAs structure, the optical absorption involves localized hole states within the QR and the continuum of electron states within the conduction band of the GaAs barrier layer. Although we initially limited the optical transitions to the Γ ($k=0$) point of the Brillouin zone, we later found that relaxing the allowed optical transitions to include states beyond the Γ -point ($k>0$) led to absorption spectra with the same characteristics as the experimental spectra. The photo-response was consequently calculated by integrating the contribution by a particular energy segment of the QR hole states (ΔE_h) and the entire distribution of conduction band states (assuming a parabolic conduction band near the Γ -point). In other words, the contribution by the QRs is treated as a band of deep centres, assuming a flat subband (heavy in-plane hole mass) for the QRs. By representing the photo-ionization cross-section of each segment, $\sigma_{\Delta E}(h\nu)$, using Lucovsky's δ -potential model,¹⁷ the spectral dependence of the internal quantum efficiency (IQE) could then be described by

$$IQE(h\nu) = \int_{\text{band}} \sigma_{\Delta E} dE_h, \quad (2)$$

$$\sigma_{\Delta E}(h\nu) = \frac{BN\sqrt{(E_g - E_h)}(h\nu - E_g + E_h)^{3/2}}{(h\nu)^3}, \quad (3)$$

where E_g is the GaAs band gap energy, E_h the hole localization energy of the band segment integrated, and $N(E_h)$ the energy distribution of the hole state density. The pre-factor B collects all the energy independent terms, with the remaining symbols having their usual meaning. The simulated photo-responses of the QR and the WL are depicted by the solid lines in Figure 1. The IQE spectrum was obtained by describing the QR height by a Gaussian distribution and adjusting the mean and full width at half maximum (FWHM) of the distribution until a good correlation with the experimental spectrum could be attained. The ΔR distribution was calculated from the height distribution by assuming a constant volume (which was estimated from the TEM result) for the QRs. Figure 2 shows the QR height distribution used to simulate the spectral response for particular choices for the valence band offset. The QR height distribution is found to vary between 1.25 and 1.45 nm for decreasing ΔE_{VB} , with the distribution broadening significantly when selecting a small band offset ($\Delta E_{VB} = 750$ meV).

Following the optimization of the QR height distribution, the associated hole energy distribution could be determined

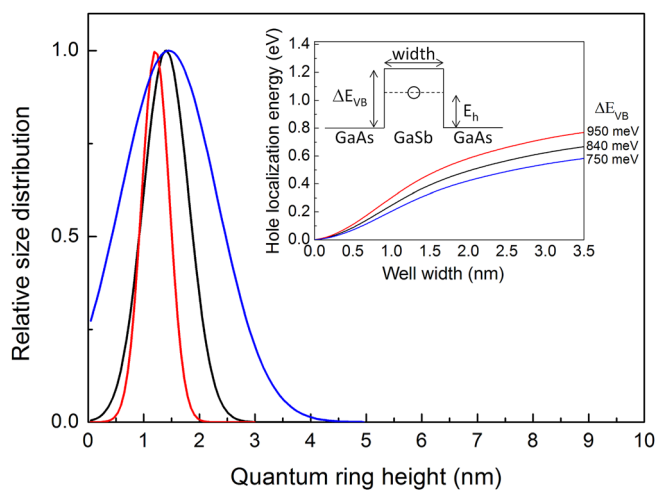


FIG. 2. Quantum ring height distribution used to simulate the extended photo-response of the GaSb/GaAs solar cell. Each distribution was calculated for a particular choice for the valence band offset. The distribution has a mean value of 1.2 nm for a band offset of 950 meV and an effective hole mass of $0.097m_0$.

concurrently. Figure 3 gives the energy distribution of the localized hole states stemming from the simulation of the QR response in Figure 1. The lines represent the energy distributions obtained with a valence band offset of 950, 840, and 750 meV. In each case, the hole localization energy associated with the radial width was used to adjust the mean of the energy distribution. Also included is the energy distribution calculated from the room temperature PL spectrum of the same sample (solid circles). Since the PL transitions would predominantly be between electron states near the conduction band minimum ($k=0$) and the localized hole states, with the hole distribution expected to be homogeneously distributed across the QRs at room temperature, the PL spectrum is expected to be a good representation of the hole energy distribution. The QR states calculated using Eqs. (2) and (3) are therefore well matched to the PL analysis when using a large valence band offset, with a Gaussian height distribution producing an asymmetric energy distribution centered 370 meV above the valence band maximum. In another study, the optical transition energies were calculated using an 8-band $\mathbf{k}\cdot\mathbf{p}$ model.⁵ However, the results only correlated with the emission energies of the PL spectra when using a much smaller valence band offset of 540 meV in their analyses. The discrepancy likely lies with an overestimation of the nano-structure size, particularly since it was estimated from atomic force microscopy performed on *uncapped* structures. In our study,

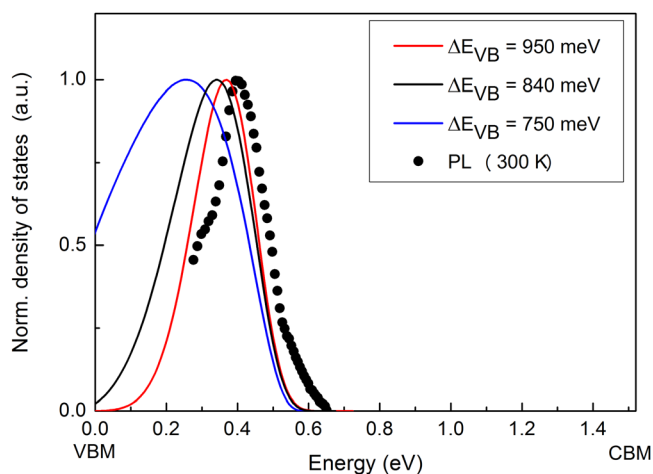


FIG. 3. Hole energy distributions emanating from the simulation of the QR related response in Figure 1. The solid circles represent the hole energy distribution estimated from the room temperature PL spectrum (i.e., band gap energy minus transition energy) of the same structure. The distribution obtained with $\Delta E_{VB} = 950$ meV (peak = 370 meV; FWHM = 220 meV) is well matched to the PL analysis.

cross-sectional TEM of the imbedded structures clearly revealed the formation of coherently strained GaSb QRs with an approximate height of 1.7 nm.¹ Although the one-dimensional representation used to relate the QR height and radial width to the hole localization energy could be viewed as an oversimplification of the quantum structure, the good agreement between the simulated height distribution for $\Delta E_{VB} = 950$ meV and the TEM results suggests that the approach, as well as the band parameters chosen, is appropriate.

Analogous to our analysis of the QR response, the thickness distribution and associated energy distribution of the WL was simulated from the IQE spectrum presented in Figure 1. Using the band parameters proposed by Pryor and Pistol⁷ for a 2-dimensional nano-structure, the WL could be described by a mean thickness and hole localization energy of 0.54 nm and 217 meV, respectively. Even though a greatly simplified valence band structure was assumed for the analysis, the estimated PL transition energy of 1.30 eV is representative of most PL reports.^{18–20}

In order to ascertain to what extent the choice in band parameters, i.e., the valence band offset and the effective hole mass effect the calculations, the height and energy distributions were compared for a range of band parameters. Figure 4 describes the dependence of the peak localization energy and QR height for different values of ΔE_{VB} . The error bars represent the distribution of the simulated distribution

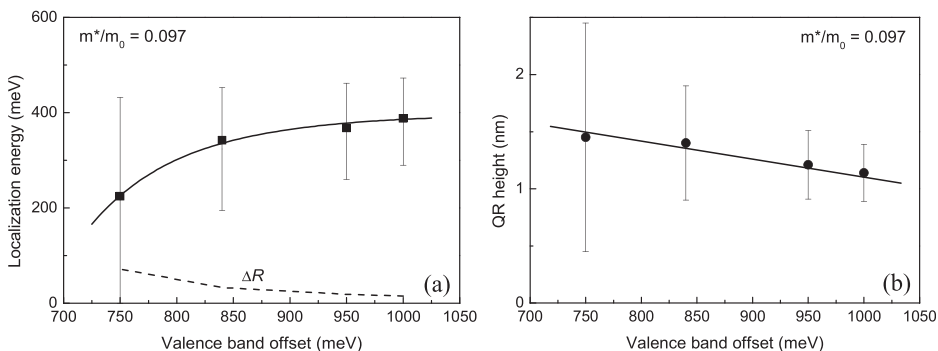


FIG. 4. The hole localization energy (a) and QR height (b) for different choices of the valence band offset. The bars represent the FWHM of each distribution. The contribution by the radial confinement energy is indicated by the dashed line. The solid lines are a guide to the eye.

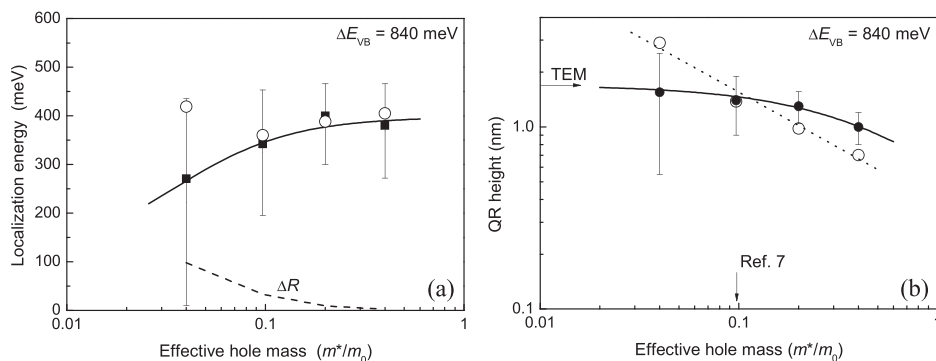


FIG. 5. The hole localization energy (a) and QR height (b) for different choices for the mean QR effective hole mass. The mismatch between the GaAs and GaSb effective hole masses were considered when calculating the solid symbols, and neglected for the open symbols. An effective hole mass of $0.082m_0$ was used for the GaAs barrier. The bars represent the FWHM of each distribution. The contribution by the radial confinement energy is indicated by the dashed line in (a). The solid lines are guide to the eye.

determined for each case. Also included is the radial confinement energy (dashed line) used to calculate the total hole localization energies using Eq. (1). As illustrated in Figures 2 and 3, small values for ΔE_{VB} result in broad distributions, with the mean QR height relatively insensitive to the choice in ΔE_{VB} . The peak localization energy also increases systematically with increasing confinement, approaching 400 meV for a large valence band offset. Since we have assumed a constant QR volume when relating the ΔR and H distributions, it is clear that radial confinement only contributes when the two distributions start to overlap, i.e., for large values of H . The role of the effective hole mass was also considered whilst keeping ΔE_{VB} constant. Figure 5 depicts the dependence of the peak localization energy and QR height (well width) for a range of values for the mean effective hole mass within the QR. The solid symbols describe the calculated values when the hole-mismatch between the well and barrier has been considered, whereas the mismatch has been neglected for the open symbols. In both cases, the simulated hole energy distributions remain relatively unchanged, deviating only for $m^* = 0.04m_0$. In the case of the height distributions, the increasing hole mismatch relative to the GaAs barrier (solid circles) leads to narrower height distributions, whereas a $1/\sqrt{m^*}$ dependence (dotted line in Fig. 5(b)) is revealed for matching barrier/well hole masses (open circles). By comparing the two approaches, we can deduce that opting for a slightly smaller effective mass for the GaAs barrier layer would lead to energy and height distributions better matched to the cross-sectional TEM and PL results of the quantum rings. As in Fig. 4, the calculated radial confinement energy (dashed line in Fig. 5(a)) tracks the QR height, contributing only due to the broadening of the height distribution for a small effective mass.

In conclusion, the extended photo-response associated with the localized hole states of type-II GaSb/GaAs quantum rings have been described using a model in which the nanostructures are represented by a Gaussian height distribution and a large valence band offset of 950 meV. The broad QR response has also been related to optical transitions between localized hole states ($k \neq 0$) and the conduction band continuum, with the peak state density lying roughly 390 meV above the valence band maximum. The correlation between

the simulated QR height distribution and the associated band of hole states have also been validated by TEM and PL measurements performed on the solar cell structure.

Financial support for this work was provided from EPSRC (Grant No. EP/G070334/1), as well as by the South African Research Chairs Initiative of the Department of Science and Technology, South African National Research Foundation, and NMMU.

- ¹P. J. Carrington, M. C. Wagener, J. R. Botha, A. M. Sanchez, and A. Krier, *Appl. Phys. Lett.* **101**, 231101 (2012).
- ²F. Hatami, M. Grundmann, N. N. Ledentsov, F. Heinrichsdorff, R. Heitz, J. Böhrer, D. Bimberg, S. S. Ruvimov, P. Werner, V. M. Ustinov, P. S. Kop'ev, and Zh. I. Alferov, *Phys. Rev. B* **57**, 4635 (1998).
- ³T. Nowozin, A. Marent, L. Bonato, A. Schliwa, D. Bimberg, E. P. Smakman, J. K. Garleff, P. M. Koenraad, R. J. Young, and M. Hayne, *Phys. Rev. B* **86**, 035305 (2012).
- ⁴D. Bimberg, M. Grundmann, and N. N. Ledentsov, *Quantum Dot Heterostructures* (John Wiley & Sons, Chichester, 2001).
- ⁵A. J. Martin, J. Hwang, E. A. Marquis, E. Smakman, T. W. Saucer, G. V. Rodriguez, A. H. Hunter, V. Sih, P. M. Koenraad, J. D. Phillips, and J. Millunchick, *Appl. Phys. Lett.* **102**, 113103 (2013).
- ⁶P. J. Carrington, A. S. Mahajumi, M. C. Wagener, J. R. Botha, Q. Zhuang, and A. Krier, *Physica B* **407**, 1493 (2012).
- ⁷C. E. Pryor and M.-E. Pistol, *Phys. Rev. B* **72**, 205311 (2005).
- ⁸C. G. Van de Walle, *Phys. Rev. B* **39**, 1871 (1989).
- ⁹J. Hwang, A. J. Martin, J. M. Millunchick, and J. D. Phillips, *J. Appl. Phys.* **111**, 074514 (2012).
- ¹⁰S.-H. Wei and A. Zunger, *Appl. Phys. Lett.* **72**, 2011 (1998).
- ¹¹Y.-H. Li, A. Walsh, S. Chen, W.-J. Yin, J.-H. Yang, J. Li, J. L. F. Da Silva, X. G. Gong, and S.-H. Wei, *Appl. Phys. Lett.* **94**, 212109 (2009).
- ¹²P. Harrison, *Quantum Wells, Wires, and Dots* (John Wiley & Sons, Ltd., Chichester, 2005), pp. 36–38.
- ¹³S. Viefers, P. Koskinen, P. Singha Deo, and M. Manninen, *Physica E* **21**, 1 (2004).
- ¹⁴I. Filikhin, E. Deyneka, and B. Vlahovic, *Modell. Simul. Mater. Sci. Eng.* **12**, 1121 (2004).
- ¹⁵R. Timm, H. Eisele, A. Lenz, L. Ivanova, G. Balakrishnan, D. L. Huffaker, and M. Dähne, *Phys. Rev. Lett.* **101**, 256101 (2008).
- ¹⁶P. Offermans, P. M. Koenraad, J. H. Wolter, D. Granados, J. M. García, V. M. Fomin, V. N. Gladilin, and J. T. Devreese, *Appl. Phys. Lett.* **87**, 131902 (2005).
- ¹⁷G. Lucovsky, *Solid State Commun.* **3**, 299 (1965).
- ¹⁸K. Suzuki, R. A. Hogg, and Y. Arakawa, *J. Appl. Phys.* **85**, 8349 (1999).
- ¹⁹M.-C. Lo, S.-J. Huang, C.-P. Lee, S.-D. Lin, and S.-T. Yen, *Appl. Phys. Lett.* **90**, 243102 (2007).
- ²⁰D. A. Álvarez, B. Alén, J. M. García, and J. M. Ripalda, *Appl. Phys. Lett.* **91**, 263103 (2007).